Available online at www.sciencedirect.com
ScienceDirect
Mendeleev Commun., 2011, 21, 215–217

Mendeleev Communications

# Investigation into the combustion of lean hydrogen–air mixtures at atmospheric pressure by means of high-speed cinematography[†]

**Nikolai M. Rubtsov,*[a] Vyacheslav D. Kotelkin,[b] Boris S. Seplyarskii,[a]**
**Victor I. Chernysh[a] and Georgii I. Tsvetkov[a]**

[a] *Institute of Structural Macrokinetics and Materials Science, Russian Academy of Sciences, 142432 Chernogolovka, Moscow Region, Russian Federation. Fax: +7 495 962 8025; e-mail: nmrubtss@mtu-net.ru*
[b] *Department of Mechanics and Mathematics, M. V. Lomonosov Moscow State University, 119991 Moscow, Russian Federation. Fax: +7 495 939 2090; e-mail: kotelkin@mech.math.msu.su*

DOI: 10.1016/j.mencom.2011.07.015

**A lean hydrogen–air ($H_2$ < 10%) mixture can be repeatedly ignited. Numerical simulation based on Boussinesq approximation is in qualitative agreement with the observed features of combustion.**

The use of hydrogen as fuel is limited by high flammability of its mixtures with air. The combustion of lean $H_2$–air mixtures in the vicinity of the lower concentration flame propagation limit (CFPL) is of particular interest. In the mixtures, the flame front (FF) is nonuniform due to high $H_2$ diffusivity. It leads to the occurrence of cellular flames[1–4] even if gravity is missing.[5] In an upward direction of flame propagation, CFPL in a lean mixture is lower than that in a downward direction;[3] $H_2$ consumption is incomplete. It is of interest to establish concentration areas of lean mixtures, in which either thermo-diffusive instability or hydrodynamic instability of FF under gravity is the controlling factor. In this work, high-speed colour cinematography was used for this purpose. As distinct from shlieren cinematography,[5] by which only the area of a drastic change in the gas density in FF is recorded, this method is more sensitive because FF emission intensity is determined by the occurrence of nonequilibrium concentrations of active particles in flame.

The numerical analysis of the system of three-dimensional balance equations for mass, momentum and thermal energy for compressible medium along with chemical kinetics equations not always provides a single valued description of gaseous combustion; *e.g.*, it depends on the choice of the model of turbulence flow.[4] The aim of this work was to study the initiated ignition of lean $H_2$–air mixtures at 1 atm by high-speed colour cinematography and to perform a numerical simulation of the process under the Boussinesq approximation to describe natural convection.[6,7]

The experiments were performed with mixtures of 4% $CCl_4$ + 7.5% $H_2$ + 88.5% air, 4% $CCl_4$ + 8% $H_2$ + 88% air and 4% $CCl_4$ + 11% $H_2$ + 85% air.[‡] The results of filming the FF propagation for these mixtures at $T$ = 298 K and spark energy of $E_0$ = 1.5 J are shown in Figure 1. In the combustion of mixtures (7.5 and 8% $H_2$ in air), the movement of FF to the top of the reactor [Figure 1(*a*),(*b*)] was observed. It was shown that after flame quenched itself after propagating, the second flame propagation in the mixture can be initiated once again at the same place by the spark of the same energy [frame 40, Figure 1(*a*), and frame 39, Figure 1(*b*)]. We observed three successive ignitions of the same mixture. As fol-

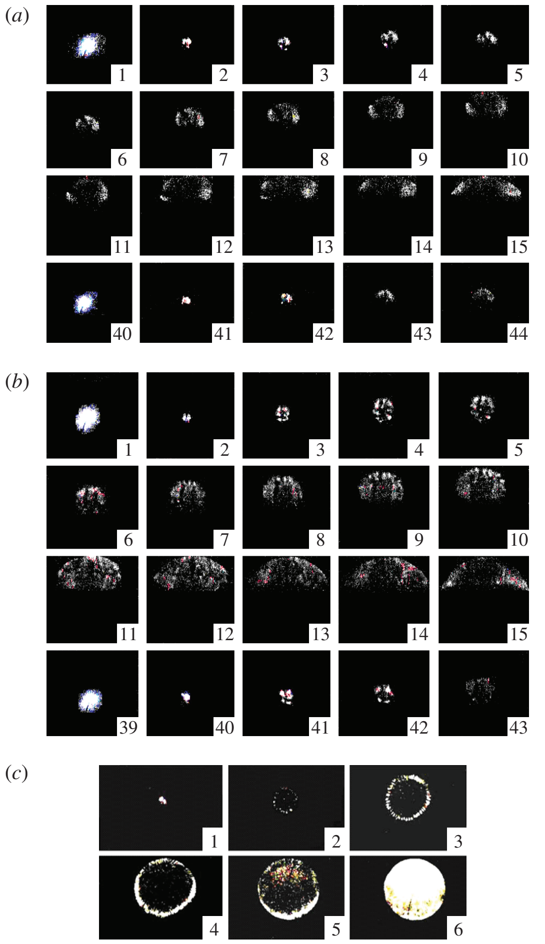

**Figure 1** Sequences of video images of the propagation of cellular FF (with consecutive numbers). 60 frames per second. (*a*) 4% $CCl_4$ + 7.5% $H_2$ + 88.5% air, (*b*) 4% $CCl_4$ + 8% $H_2$ + 88% air and (*c*) 4% $CCl_4$ + 11% $H_2$ + 85% air; $T_0$ = 298 K, $E_0$ = 1.5 J. To start playback of the video clip available in the electronic version of the article, click on any image of Figure 1(*c*).

---

[†] The electronic version of this article includes a video clip for Figure 1(*c*).

[‡] 4% of carbon tetrachloride ($CCl_4$) was added for the visualization of FF. Note that the $CCl_4$ additive up to 5% to lean $H_2$–air mixtures does not show any inhibiting action on combustion.[5] A horizontal stainless steel reactor 25 cm in length and 12 cm in diameter supplied with demountable covers and an optical window 10 cm in diameter at a butt-end was used in the experiments.[8] Electrodes of spark ignition were mounted at the reactor centre. Gas mixture was formulated in the reactor. First, $CCl_4$ vapour and then $H_2$ and air were allowed to bleed into the reactor to 1 atm. Spark initiation was carried out in 20 min. Ignition and FF propagation were recorded by means of a Casio Exilim F1 Pro colour high speed Full HD camera with a speed of 60 frames per second. Before each experiment, the reactor was pumped to $10^{-2}$ Torr.

lows from the calculations below, the number of repeated ignitions increases with the reactor volume. At the repeated initiation quantity of cells and FF velocity are approximately the same as at the first ignition. The result indicates the necessity to account for the repeated ignition in lean $H_2$–air mixtures under development of fire control systems. It was also established that, in the richest mixture (11% $H_2$ + 89% air), cellular FF extends in all directions practically with the same velocity [Figure 1(*c*)], and faster by a factor of 4 than that in the mixtures containing 7.5 and 8% $H_2$ in air [Figure 1(*a*),(*b*)]. This result suggests that at the concentration of $H_2$ higher than 10%, the flame velocity increases so that natural convection has no effect on FF velocity in upward direction. Note that, in such mixtures burning 'symmetrically', repeated FF propagation is not observed.

At numerical simulation we considered a flat two-dimensional system of equations where the reaction-diffusion system is coupled with the Navier–Stokes equations under the Boussinesq approximation to describe natural convection, which can occur because of the heat produced by the reaction.[6,7] In this model, changes in density $\rho$ are caused by changes in temperature $T$ ($\rho_0$ is the initial density, and $\beta$ is the factor of volume expansion of the medium):

$$\rho = \rho_0 + \delta\rho, \quad \delta\rho << \rho_0, \quad \delta\rho = -\rho_0\beta T. \tag{1}$$

Density change is considered only in the equations of movement and ignored in the indissolubility equation. Then (after subtraction of hydrostatic pressure $p_0 = \rho_0 gh$), two-dimensional equations of movement and indissolubility in dimensionless variables $\xi = x/L_0$, $\zeta = y/L_0$, $\tau = t/t_0$, $\vartheta = u/V_0$, $v = \upsilon/V_0$, $\theta = (T - T_0)/(T_c - T_0)$, $\pi = p/P_0$, $Y_i = C_i/[H_2]_0$, where $L_0$, $t_0$, $V_0$, $T_0$, $P_0$ are characteristic dimensional scales of length, time, speed, temperature and pressure, $C_i$ is the concentration of components, $g$ = 980 cm s$^{-1}$, $u$, $\upsilon$ are the components of current velocity, $T_c$ is the adiabatic combustion temperature of the mixture of given composition, and $T_0$ is the initial temperature, take the form:

$$\mathrm{Re}\left(\frac{\partial\bar{V}}{\partial\tau} + \vartheta\frac{\partial\bar{V}}{\partial\xi} + v\frac{\partial\bar{V}}{\partial\zeta}\right) = -\bar{\nabla}\pi + e_y\mathrm{Ra}\theta + \Delta\bar{V}, \quad \bar{\nabla}\bar{V} = 0, \tag{2}$$

where $\bar{V} = V(u,v)$ is the medium velocity, and $e_y$ is the unit vector in upward direction. Temperature distribution in gas is described by the heat conductivity equation ($\chi$ is thermal diffusivity and $Q_i$ is heat emission sources)

$$\frac{\partial\theta}{\partial\tau} + \vartheta\frac{\partial\theta}{\partial\xi} + v\frac{\partial\theta}{\partial\zeta} = \frac{1}{\mathrm{Pe}_T}\Delta\theta + \sum Q_i. \tag{3}$$

Distributions of component concentration are described by the corresponding reaction-diffusion equations ($D_i$ is diffusivity and $K_{ij}$ is rate constant)

$$\frac{\partial Y_i}{\partial\tau} + \vartheta\frac{\partial Y_i}{\partial\xi} + v\frac{\partial Y_i}{\partial\zeta} = \frac{1}{\mathrm{Pe}_i}\Delta Y_i + \sum_{i,j} K_{ij}Y_i. \tag{4}$$

In equations (2)–(4),[§] traditional notations for dimensionless numbers of Rayleigh (Ra), Reynolds (Re) and Pecle ($\mathrm{Pe}_T$, $\mathrm{Pe}_i$) were used.

$$\mathrm{Ra} = \frac{\rho_0 g\beta T_0 L_0^3}{\eta\chi}, \quad \mathrm{Re} = \frac{\rho_0 L_0 V_0}{\eta}, \quad \mathrm{Pe}_T = \frac{L_0 V_0}{\chi}, \quad \mathrm{Pe}_i = \frac{L_0 V_0}{D_i}. \tag{5}$$

The objective consisted in the establishment of the possibility of qualitative modeling of both cellular combustion regime and increase in cells quantity with increase of $H_2$ content, as well as repeated initiation of a cellular flame in the mixture, which already burnt. The reduced kinetic mechanism of $H_2$ combustion at 1 atm was represented in the form[13]

$\mathrm{H_2 + O_2 \rightarrow 2OH}$, $k_0 = 1.92\times10^{14}\exp(-21890/T)$ cm$^3$ molec$^{-1}$ s$^{-1}$,[14]
$\mathrm{OH + H_2 \rightarrow H_2O + H}$, $k_1 = 4.63\times10^{12}\exp(-2100/T)$ cm$^3$ molec$^{-1}$ s$^{-1}$,[15]
$\mathrm{H + O_2 \rightarrow OH + O}$, $k_2 = 1.99\times10^{14}\exp(-8460/T)$ cm$^3$ molec$^{-1}$ s$^{-1}$,[16]
$\mathrm{O + H_2 \rightarrow OH + H}$, $k_3 = 1.88\times10^{14}\exp(-6897/T)$ cm$^3$ molec$^{-1}$ s$^{-1}$,[16]
$\mathrm{H + O_2 + M \rightarrow HO_2 + M}$, $k_4 = 6.47\times10^{15}(T/298)^{-0.8}$ cm$^6$ molec$^{-2}$ s$^{-1}$,[17]
$\mathrm{H + HO_2 \rightarrow 2OH}$, $k_5 = 1.69\times10^{14}\exp(-440/T)$ cm$^3$ molec$^{-1}$ s$^{-1}$,[16]
$\mathrm{H_2 + HO_2 \rightarrow H_2O_2 + H}$, $k_6 = 3\times10^{13}\exp(-14400/T)$ cm$^3$ molec$^{-1}$ s$^{-1}$,[16]
$\mathrm{OH + O \rightarrow H + O_2}$, $k_7 = 9.29\times10^{12}$ cm$^3$ molec$^{-1}$ s$^{-1}$,[18]
$\mathrm{O + HO_2 \rightarrow OH + O_2}$, $k_8 = 3.25\times10^{13}$ cm$^3$ molec$^{-1}$ s$^{-1}$,[16]
$\mathrm{OH + HO_2 \rightarrow H_2O + O_2}$, $k_9 = 2.89\times10^{13}\exp(250/T)$ cm$^3$ molec$^{-1}$ s$^{-1}$,[17]
$\mathrm{2HO_2 \rightarrow H_2O_2 + O_2}$, $k_{10} = 2\times10^{12}$ cm$^3$ molec$^{-1}$ s$^{-1}$,[19]
$\mathrm{H_2O_2 + M \rightarrow 2OH + M}$, $k_{11} = 1.3\times10^{17}\exp(-22750/T)$ cm$^3$ molec$^{-1}$ s$^{-1}$,[20]
$\mathrm{H + H + M \rightarrow H_2 + M}$, $k_{12} = 2.2\times10^{15}$ cm$^6$ molec$^{-2}$ s$^{-1}$.[17]

Dimensionless time scales, lengths and speeds of process were chosen as follows: $t_0 = 1/(k_1^0[H_2]_0)$, $x_0 = y_0 = (D_3/k_1^0[H_2]_0)^{1/2}$, $V_0 = x_0/t_0 = (D_3k_1^0[H_2]_0)^{1/2}$, $\delta_4 = \chi/D_3$, where $k_1^0 = 4.63\times10^{12}$ is the preexponential factor of reaction $\mathrm{OH + H_2 \rightarrow H_2O + H}$, $D_3$ is the $H_2$ diffusivity. Dimensionless variables and parameters took the form $\tau = t/t_0$, $\xi = x/x_0$, $\zeta = y/y_0$, $Y_i = c_i/[H_2]_0$ ($c_i$ is the concentration of $i$th component). $K_\mathrm{p}$ is the dimensionless reaction velocity. For a bimolecular step, $K_\mathrm{p} = k_\mathrm{p}/k_1^0 p$ corresponds to the step number ($p \neq 4, 12$). For a termolecular step, $K_p = k_p[H_2]_0/k_1^0$, where $p = 4, 12$. Nondimensional diffusivities $\delta_0$, $\delta_1$, $\delta_2$, $\delta_3$, $\delta_5$, $\delta_6$, $\delta_7$ ($\delta_i = D_i/D_3$, $i$ = 0–6) in $H_2$–air mixture correspond to OH, O, H, $H_2$,$O_2$, $HO_2$ and $H_2O_2$, respectively. For example, the heat conductivity equation in dimensionless variables takes the form:

$$\frac{\partial\theta}{\partial\tau} + \vartheta\frac{\partial\theta}{\partial\xi} + v\frac{\partial\theta}{\partial\zeta} = \delta_4\left(\frac{\partial^2\theta}{\partial\xi^2} + \frac{\partial^2\theta}{\partial\zeta^2}\right) + \frac{[H_2]_0}{C_p\rho(T_c - T_0)}\sum_p\sum_{m,n} Q_pK_pY_mY_n.$$

Here, $C_p$ is the average thermal capacity at constant pressure, 0.25 cal g$^{-1}$ K$^{-1}$;[21] $\delta_4$ is nondimensional thermal diffusivity of the mixture, it is considered that $\delta_4 \approx \delta_5$, $\rho$ is gas density (g cm$^{-3}$), $M = 760\times10^{19}/T$, $T$ is temperature (K). Thermal effects of elementary steps $Q_i$ and diffusivities were taken from refs. 22,23. Indexes $m,n$, which change from 0 to 6, correspond to nondimensional concentrations of OH, O, H, $H_2$, $O_2$, $HO_2$ and $H_2O_2$. The index $p$ at dimensionless rate constants $K_p = k_p/k_1^0$ changes from 0 to 12 and corresponds to the reaction number in the kinetic mechanism above. The initiation centre was given by an ellipse with axes of 20×30 nodes [Figure 2(*a*),(*b*)], in which nondimensional H atoms concentration and $\theta$ were set equal to 0.4–0.6. In the calculated area outside of the centre of ignition the concentration of all intermediates were set equal to zero, $\theta = 0$, concentration of $H_2$ was set equal to 6 and 8% in air containing 21% $O_2$. Thus, the solution of the system of equations (2)–(4) satisfies the following initial conditions outside of initiation area: $0 < \xi < L$, $0 < \zeta < L$, $\tau = 0$: $Y_i(0,\xi,\zeta) = 0$ ($i \neq 3,4$), $Y_3(0,\xi,\zeta) = f_{H_2}$, $Y_4(0,\xi,\zeta) = {}$ $= f_{O_2}$, $T(0,\xi,\zeta)$ = 300 K. Boundary conditions are $0 < \xi < L$: $T(\tau,\xi,0)$ = 300 K, $T(\tau,\xi,L)$ = 300 K, $0 < \zeta < L$: $T(\tau,0,\zeta)$ = 300 K, $T(\tau,L,\zeta)$ = 300 K. On the boundaries the termination of active centres is missing: $[\partial Y_i(\tau,\xi,\zeta)/\partial\zeta]_L = 0$, $[\partial Y_i(\tau,\xi,\zeta)/\partial\xi]_L = 0$, where $L$ is dimensionless length and width of the channel, corresponding to dimensional size of 5.9 cm under our conditions,

---

[§] Calculations were performed in Cartesian coordinates using a uniform grid (513×513 nodes). The second order of approximation of finite difference derivatives was used. Integration of equation (2) was performed in two stages.[9] At first, the movement equations were integrated without pressure forces, and intermediate field of velocities was obtained, then from indissolubility condition a potential additive to the intermediate field of velocities, corresponding to the action of a pressure gradient was calculated. Pressure field was calculated by solving a boundary problem with the use of multigrid techniques[11] for equation (2), which turns out from indissolubility condition as a result of substitution of the intermediate field of speeds.[10] After computation of the field of speeds, numerical integration of equations (3), (4) was performed to calculate new values of temperature and concentration. On lateral borders of the calculated area normal derivatives were put equal to zero (a condition of mirror symmetry). The integration of equations (3), (4) was carried out by a modified alternately triangular method.[12]

$f_{H_2}, f_{O_2}$ are the fractions of initial reagents ($[H_2]_0$ and $[O_2]_0$) in the mixture.

Calculated profiles of H atoms in FF for $[H_2]_0 = 6\%$ and $[H_2]_0 = 8\%$ are shown in Figure 2(*a*) and 2(*b*), respectively. The shade of gray colour in Figure 2 defines the value of H atoms concentration, more light colour corresponds to a higher concentration. Note that the best agreement with experimental data presented in Figure 1 is reached at $[H_2]_0 = 4\%$ and $[H_2]_0 = 6\%$, respectively. For the kinetic scheme above, the value of lower CFPL at 1 atm is 2%. The value is in qualitative agreement with published data,[3] where it is shown that, in an upward direction of flame propagation, CFPL is lower than that in a downward direction. It is known[24] that the value of CFPL can even reach 3% depending on both spark power and recording procedure. The model used in this work does not describe the regime of cellular FF propagation in all directions practically with the same velocity [Figure 1(*c*)] for $[H_2]_0 > 10\%$, namely, the influence of convection is noticeable. The result obtained specifies the applicability of the Boussinesq approximation to the analysis of flame propagation in lean $H_2$–air mixtures as $[H_2]_0$ increases.

As is seen in Figure 2, the calculations allowed us to qualitatively describe both cellular regimes of combustion and an increase in cells quantity as $[H_2]_0$ rose for mixtures with $[H_2]_0 < 8\%$. In addition, the possibility of repeated initiation of cellular flame in a mixture, which has already burnt [frame 12 in Figure 2(*a*) and frame 11 in Figure 2(*b*)] is due to the movement of both FF and hot reaction products to the top of the reactor. It leads to the enrichment of a bottom part of the reactor in $H_2$; therefore, the gas mixture becomes combustible. The aforesaid is illustrated by Figure 3, in which the calculations of $H_2$ concentration in the course of cellular FF propagation, corresponding to frames 12–16 in Figure 2(*a*), are presented. Note that the results of calculations are in qualitative agreement with the theory of thermo-diffusive instability of flames.[2,3] Thus, if all diffusivities are put equal to each other and to thermal diffusivity (thermo-diffusive instability is missing) propagation of a smooth flame ‘upwards’ rather than cellular regimes of combustion shown in Figure 2 is observed in calculations.

Influence of the chemical nature of the most quickly diffusing particle on the features of lean $H_2$–air flames propagation was investigated numerically. The diffusivity of OH radicals in calculations was put equal to the diffusivity of H atoms; simultaneously, the diffusivity of H atoms was put equal to the diffusivity of OH radicals; *i.e.*, OH radicals became the most quickly diffusing particles. However, neither the cellular character of a flame nor its velocity considerably changed. It means that, within the limitations of calculations performed, the regularities of lean hydrogen flames propagation do not depend on the nature of the most quickly diffusing intermediate product, and they are determined by the diffusivity of the initial insufficient component.[2,3]

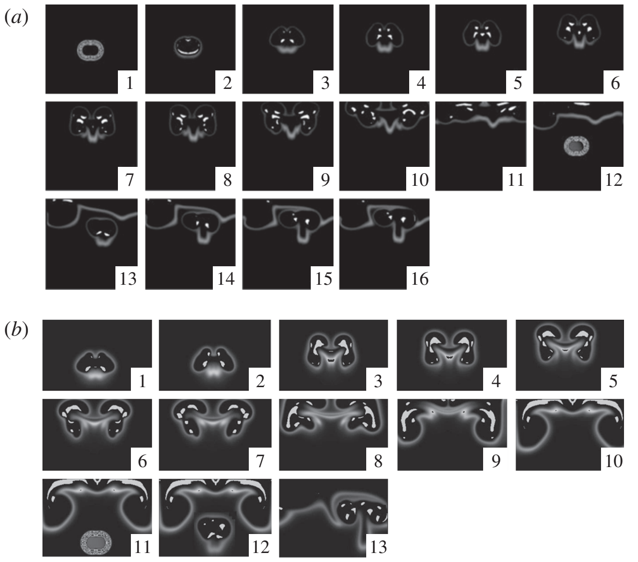

**Figure 2** Numerical simulations of the cellular FF propagation. (*a*) 6% $H_2$ + 94% air, $T_0 = 298$ K. Time interval between frames 1–11, 12–16 is ~0.04 s, between frames 8 and 9, 0.5 s. (*b*) 8% $H_2$ + 92% air, $T_0 = 298$ K. Time interval between frames 1–10, 11–13 is ~0.01 s, between frames 10 and 11, 0.5 s.

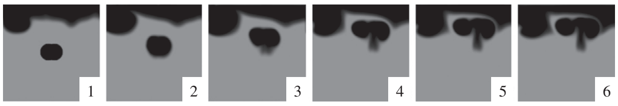

**Figure 3** Numerical simulation of $H_2$ concentration in cellular FF, corresponding to frames 12–16 in Figure 2(*b*). 6% $H_2$ + 94% air, $T_0 = 298$ K.

This work was supported by the Russian Foundation for Basic Research (project no. 10-08-00305a).

## References

1 F. A. Williams and J. F. Grcar, *Proc. Combust. Instit.*, 2009, **32**, 1351.

2 Ya. B. Zel’dovich, G. I. Barenblatt, V. B. Librovich and G. M. Machviladze, *Matematicheskaya teoriya goreniya i vzryva (Mathematical Theory of Combustion and Explosion)*, Nauka, Moscow, 1980 (in Russian).

3 Ya. B. Zel’dovich, *Izbrannye trudy, Chimicheskaya fizika i gidrodinamika (Selected Works, Chemical Physics and Hydrodynamics)*, Nauka, Moscow, 1980 (in Russian).

4 V. V. Molkov, D. V. Makarov and H. Schneider, *J. Phys. D: Appl. Phys.*, 2006, **39**, 4366.

5 P. D. Ronney, *Combust. Flame*, 1990, **82**, 1.

6 J. W. Rayleigh, *Phil. Mag.*, 1916, **32**, 529.

7 L. D. Landau and E. M. Lifshits, *Teoreticheskaya fizika, Vol. 6. Gidrodinamika (Theoretical Physics. Vol. 6. Hydrodynamics)*, Nauka, Moscow, 1986 (in Russian).

8 N. M. Rubtsov, B. S. Seplyarskii, V. I. Chernysh and G. I. Tsvetkov, *Mendeleev Commun.*, 2008, **18**, 105.

9 A. J. Chorin, *J. Comput. Phys.*, 1967, **2**, 12.

10 G. I. Marchuk, *Metody vychislitel’noi matematiki (Methods of Computational Mathematics)*, Nauka, Moscow, 1989 (in Russian).

11 P. Wesseling, *An Introduction to Multigrid Methods*, Wiley, New York, 1992.

12 A. A. Samarskii and A. V. Gulin, *Chislennye metody matematicheskoi fiziki (Numerical Methods of Mathematical Physics)*, Nauchnyi Mir, Moscow, 2000 (in Russian).

13 N. M. Rubtsov, B. S. Seplyarskii, V. I. Chernysh and G. I. Tsvetkov, *Mendeleev Commun.*, 2008, **18**, 220.

14 V. V. Azatyan, E. N. Alexandrov and A. F. Troshin, *Kinet. Katal.*, 1975, **16**, 306 [*Kinet. Catal.* (*Engl. Transl.*), 1975, **16**, 346].

15 R. Atkinson, D. L. Baulch, R. A. Cox, R. F. Hampson, Jr., J. A. Kerr, M. J. Rossi and J. Troe, *J. Phys. Chem. Ref. Data*, 1997, **26**, 1329.

16 D. L. Baulch, C. J. Cobos, R. A. Cox, C. Esser, P. Frank, Th. Just, J. A. Kerr, M. J. Pilling, J. Troe, R. W. Walker and J. Warnatz, *J. Phys. Chem. Ref. Data*, 1992, **21**, 411.

17 S.-O. Ryu, S. M. Hwang and M. J. Rabinowitz, *Chem. Phys. Lett.*, 1995, **242**, 279.

18 D. L. Baulch, C. T. Bowman, C. J. Cobos, R. A. Cox, Th. Just, J. A. Kerr, M. J. Pilling, D. Stocker, J. Troe, W. Tsang, R.W. Walker and J. Warnatz, *J. Phys. Chem. Ref. Data*, 2005, **34**, 566.

19 H. Yang, W. C. Gardiner, K. S. Shin and N. Fujii, *Chem. Phys. Lett.*, 1994, **231**, 449.

20 Y. K. Park and D. G. Vlachos, *J. Chem. Soc., Faraday Trans.*, 1998, **94**, 735.

21 *Tablitsy fizicheskikh velichin (Tables of Physical Values)*, ed. I. K. Kikoin, Atomizdat, Moscow, 1976, p. 1007 (in Russian).

22 B. D. Hitch and D. W. Senser, *AIAA-1988-732, Aerospace Sciences Meeting*, 11–14 Jan 1988, Reno, NV, USA, p. 11.

23 A. A. Konnov, *Khim. Fiz.*, 2004, **23**, 5 [*Chem. Phys. Rep.* (*Engl.Transl.*), 2004, **23**, 10].

24 K. L. Cashdollar, I. A. Zlochower, G. M. Green, R. A. Thomas and M. Hertzberg, *J. Loss Prev. Process Ind.*, 2000, **13**, no. 3–5, 327.

*Received: 4th January 2011; Com. 11/3661*